

## Fluid-absent diffusion kinetics of Al inferred from retrograde metamorphic coronas

JOHN R. ASHWORTH

School of Earth Sciences, University of Birmingham, Edgbaston, Birmingham B15 2TT, U.K.

### ABSTRACT

Estimates are obtained for diffusion coefficients of Al through polycrystalline hornblende layers during retrograde metamorphism using petrological studies of two types of coronas, with geologically based estimates of time scale. The observations indicate a combination of fluid-absent grain-boundary diffusion and intracrystalline diffusion in the presence of composition gradients whose magnitude for Al is constrained by mineral analyses. Corona growth is linked to diffusion by the results of steady-state modeling of the diffusion-controlled reaction. The estimated effective (bulk) diffusion coefficient  $D_{Al}^{eff}$  is  $10^{(-24 \pm 2)}$  m<sup>2</sup>/s, leading to a maximum estimate for the product of grain-boundary diffusion coefficient  $D_{Al}^{gb}$  and grain-boundary width,  $\delta$ , of  $10^{(-29 \pm 2)}$  m<sup>3</sup>/s. In comparison with data in the literature,  $D_{Al}^{eff}$  is greater (by up to a few orders of magnitude) than intracrystalline Al diffusion coefficients (extrapolated from high-temperature experiments), as expected where grain-boundary diffusion is important. However,  $D_{Al}^{eff}$  is smaller than would be expected if grain boundaries had high contents of dissolved H<sub>2</sub>O. The results are consistent with H<sub>2</sub>O concentration being an important kinetic control on retrograde reaction.

### INTRODUCTION

Mineralogical layering produced by metamorphism is characteristic of diffusion-controlled reaction (Fisher, 1978). Using the principles of steady-state diffusion of oxide components (e.g., AlO<sub>3/2</sub>, MgO) with local equilibrium (Fisher, 1973), Joesten (1977) modeled the development of layers between two reactant minerals. An open-system extension of the method (Ashworth and Birdi, 1990) is applicable to layered coronas (e.g., Fig. 1), with the complication that the reaction changes during the growth of some coronas (Johnson and Carlson, 1990; Carlson and Johnson, 1991). Although interdiffusion of several major elements is involved, the modeling clearly implies different mobilities among the cation-forming elements. In the examples studied by Ashworth and Birdi (1990) and Ashworth et al. (1992), although the overall reaction progress is controlled by components with relatively large diffusive fluxes, the distribution of minerals among layers is strongly influenced by the relatively immobile elements Al and Si. Restricted diffusion of Al, in particular, produces an Al-rich layer (adjacent to the Al-rich reactant mineral, plagioclase), separated from an Al-poor layer (adjacent to reactant olivine or pyroxene) by a thin transition layer (Fig. 1) with intermediate Al content.

The modeling has no absolute time scale, and does not use concentration gradients (it implicitly relies on relative chemical-potential gradients). However, the transition layer suggests a gradient in Al concentration between the Al-rich and Al-poor layers. A rough estimate of diffusion coefficient  $D_{Al}$  (m<sup>2</sup>/s), for comparison with other diffusion

studies, can be obtained from Fick's first law,

$$J_i = -D_i \frac{dc_i}{dx} \quad (1)$$

if the gradient  $dc_{Al}/dx$  (mol/m<sup>4</sup>) can be constrained along with the time scale for the flux  $J_{Al}$  (mol/m<sup>2</sup>s) through the transition layer.

Equation 1 strictly applies to diffusion through a particular medium. If this is an aqueous fluid in grain boundaries, concentration gradients are small, but diffusion coefficients are so much greater than in solids that diffusion through the fluid should be dominant. Walther and Wood (1984) argued for this process during prograde metamorphism in which H<sub>2</sub>O is produced by dehydration reactions. On the other hand, the corona-forming reactions of Ashworth and Birdi (1990) and Ashworth et al. (1992) are retrograde and consume H<sub>2</sub>O. Their small scale (commonly ~100 μm, Fig. 1) compared with domains of diffusion-controlled reaction during prograde dehydration (commonly 1–10 mm: e.g., Foster, 1977) suggests that diffusion in the coronas was hindered by fluid absence (cf. Walther and Wood, 1984). If aqueous fluid infiltrated along fractures, the distribution of hydration products should be nonuniform (localized near the fractures: Rubie, 1986; Carlson and Johnson, 1991), whereas, in the rocks studied here, coronas grew at all contacts between the reactant minerals. It is very unlikely that a fluid phase penetrated all the grain boundaries within the corona (Fig. 1), yet the component H<sub>2</sub>O was pervasively available for hydration reactions at internal contacts between layers. This is explained by diffusion of H<sub>2</sub>O from fractures to

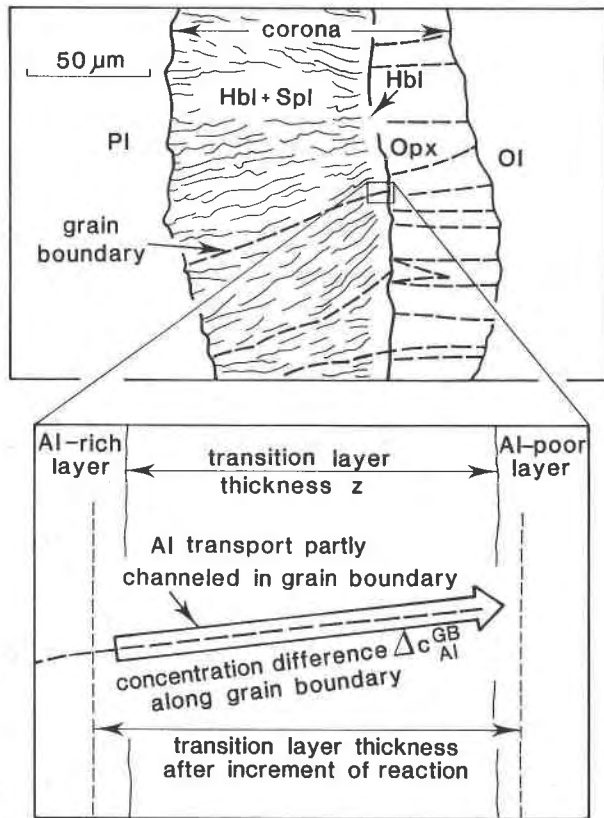


Fig. 1. Petrographic sketch of the layer structure of a corona (specimen 53P of Ashworth and Birdi, 1990) and diagram to illustrate growth accompanied by diffusion. The transition layer has an Al content intermediate between the Al-rich layer adjacent to the Al-rich reactant mineral (plagioclase) and Al-poor layer adjacent to olivine. During an increment of reaction, growth of the layer is coupled with diffusion through it, whereby Al diffuses toward the Al-poor layer. Part of this flux is pictured as channeled in the grain boundary rather than being volume diffusion through the bulk hornblende.

coronas and through them:  $H_2O$  was a fast-diffusing component in the open system.

Solid-state diffusion is consistent with the inferred immobility of Al relative to the large-flux elements, Mg and Fe in coronas around olivine (Ashworth and Birdi, 1990) and Ca around clinopyroxene (Ashworth et al., 1992), since Al is a slow-diffusing cation in experimental studies of intracrystalline diffusion (Sautter et al., 1988a). By comparison, Foster (1981) inferred relatively mobile behavior of Al in a prograde, possibly fluid-present reaction.

In addition to intracrystalline diffusion (also called volume or lattice diffusion), grain-boundary diffusion is possible in the solid state. The grain boundary can provide an easier route for diffusion than the crystal interior ( $D_{gb}^{Al} > D_{vol}^{Al}$ ), particularly at low temperatures, because the grain-boundary region of the crystal is disordered (Fisher and Elliott, 1974; Rubie, 1986). It can be considered as a solid-solution medium and may contain relatively high

concentrations of diffusion-catalyzing components, notably  $H_2O$  (Rubie, 1986). During corona-forming reactions studied by Ashworth et al. (1992), volume diffusion operated to produce both epidote inclusions clouding plagioclase and zoned amphibole in some Al-poor layers of coronas (Al-rich rims  $\sim 1 \mu m$  wide adjacent to grain boundaries, surrounding Al-poor cores of grains). Diffusion along grain boundaries is also indicated, which produces corona growth on a scale of  $\sim 100 \mu m$  without obvious intracrystalline concentration gradients for the mobile components. Many grain boundaries are available, since grain dimensions perpendicular to diffusion direction are typically 1–100  $\mu m$  (Fig. 1).

Across the thin transition layers considered here, zoning is detected only in a direction perpendicular to the layer contacts, and diffusion should be approximately unidirectional, making Equation 1 applicable. Both grain-boundary and volume diffusion of Al are expected as parallel processes, the grain-boundary flux being associated with a grain-boundary concentration gradient (Fig. 1). The quantity to be estimated is a bulk diffusion coefficient,  $D_{Al}^{eff}$ , for combined grain-boundary and volume diffusion.

#### RELATION BETWEEN MODELING AND DIFFUSION COEFFICIENTS

The modeling is one dimensional; i.e., bulk diffusive fluxes are modeled as perpendicular to planar contacts between layers. This is reasonable where coronas are thin relative to reactant grain size. Modeling gives computed fluxes through the transition layer,  $J_t^{model}$ , per unit of reaction progress  $\xi$ , associated with molar amounts of minerals  $k$  produced, which can be converted (using molar volumes  $V^k$ ) to the amount of layer growth  $G$  (symbols and units are listed in Table 1). It has been inferred by Ashworth and Birdi (1990) and Ashworth et al. (1992) that the transition layer grows at both contacts (and would contain an inert marker placed at the contact between reactant minerals before reaction: Joesten, 1977). The reference frame for diffusion is given by the instantaneous positions of the layer contacts (Nishiyama, 1983). In diffusion studies in general, fluxes depend on the choice of reference frame (Brady, 1975), and an apparent flux of a nondiffusing component may arise from bulk flow of the other components. However, in the coronas, fluxes are linked to layer-contact reactions. If the Al fluxes were spurious, the real reactions would be Al-conserving, and the intermediate Al content of the transition layer could only be an accident of fortuitous addition and subtraction of other components. It is much more likely that the transition layers, found in two quite different types of corona, are produced by Al transport toward the Al-poor layer.

The growth rate of the layer,  $dz/dt$ , and the flux,  $J_t$ , of Equation 1 are related to  $G$  and  $J_t^{model}$  by

$$\frac{dz}{dt} = \left( \frac{G}{A} \right) \frac{d\xi}{dt} \quad (2)$$

and

$$J_t = \left( \frac{J_t^{model}}{A} \right) \frac{d\xi}{dt} \quad (3)$$

In the steady-state modeling, minerals are treated as homogeneous (unzoned) phases. Nevertheless, diffusion implies concentration gradients. A reasonable assumption is that each flux  $J_i$  is constant throughout a given layer, i.e., reaction is confined to layer contacts (Joesten, 1977; Ashworth and Birdi, 1990). If, in Equation 1,  $D_i$  is also approximately constant, then so is  $dc_i/dx$ . For diffusion in medium  $k$  through a layer of thickness  $z$ ,

$$\left(\frac{dc_i}{dx}\right)^k \approx \frac{\Delta c_i^k}{z}$$

For pure volume diffusion, Equation 1 becomes

$$J_i \approx \frac{-D_i^{\text{vol}} \Delta c_i^{\text{vol}}}{z} \quad (4)$$

The concentration difference  $\Delta c_i^{\text{gb}}$  in the grain boundary may differ from  $\Delta c_i^{\text{vol}}$  (see below). Since the flux is measured per unit cross-sectional area (perpendicular to flux) of the bulk layer, it is related to concentration gradients by the bulk or effective diffusion coefficient,  $D_i^{\text{eff}}$  (Joesten and Fisher, 1988, p. 724). For pure grain-boundary diffusion,

$$J_i \approx \frac{-D_i^{\text{eff}} \Delta c_i^{\text{gb}}}{z} \quad (5)$$

For combined grain-boundary and volume diffusion, with a weighted average or effective concentration difference  $\Delta c_i^{\text{eff}}$ ,

$$J_i \approx \frac{-D_i^{\text{eff}} \Delta c_i^{\text{eff}}}{z} \quad (6)$$

of which Equations 4 and 5 are limiting cases. Combining Equations 2, 3, and 6, and integrating gives the equation used below to estimate  $D_{\text{AI}}^{\text{eff}}$ :

$$z^2 \approx \frac{-2G \Delta c_i^{\text{eff}} D_i^{\text{eff}} t}{J_i^{\text{model}}} \quad (7)$$

This is comparable with Equation 2 of Brady (1983).

For pure grain-boundary diffusion,

$$D_i^{\text{eff}} = \tau \beta D_i^{\text{gb}}$$

(symbols defined in Table 1). Tortuosity ( $\tau$ ) is discussed by Brady (1983). For straight grain boundaries approximately parallel to the bulk flux (a fair approximation in the coronas, Fig. 1),  $\tau \approx 1$  and  $\beta \approx N\delta$ . Strictly,  $\tau$  is slightly less than 1 for grain boundaries oblique to bulk flux, whereas  $N\delta$  slightly underestimates  $\beta$  (by a factor of  $\frac{1}{2}$  if grain-boundary orientation is random in the plane perpendicular to flux: Smith and Guttman, 1953). These two small uncertainties tend to cancel out. Unlike  $N$ ,  $\delta$  is not readily measured (estimates range from  $\sim 1$  to  $\sim 100$  nm: Rubie, 1986; Joesten, 1991; Farver and Yund, 1991), so the quantity usually estimated is the product  $D_i^{\text{gb}}\delta$ . This can be calculated from

$$D_i^{\text{gb}}\delta \approx \frac{D_i^{\text{eff}}}{N} \quad (8)$$

TABLE 1. Explanation of symbols and units

|   |   |
|---|---|
| $c_i^k$   | concentration of component $i$ in medium $k^*$ (mol/m <sup>3</sup> )                                    |
| $(dc_i/dx)^k$   | spatial gradient of $c_i^k$ (mol/m <sup>4</sup> )   |
| $\Delta c_i^k$  | difference in $c_i^k$ across a layer (mol/m <sup>3</sup> )  |
| $\Delta c_i^{\text{eff}}$   | effective average $\Delta c_i^k$ for combined grain-boundary and volume diffusion (mol/m <sup>3</sup> ) |
| $D_i^k$   | diffusion coefficient of component $i$ in medium $k$ (m <sup>2</sup> /s)                                |
| $D_i^{\text{eff}}$  | effective (bulk) diffusion coefficient of component $i$ (m <sup>2</sup> /s)                             |
| $J_i$   | bulk (volume + grain boundary) diffusive flux of component $i$ (mol/m <sup>2</sup> s)                   |
| $n_i^k$   | = $c_i^k V^k$ for mineral $k$ (moles of the component per mole of the mineral)                          |
| $t$   | time (s)  |
| $V^k$   | molar volume of mineral $k$ (m <sup>3</sup> /mol)   |
| $\beta$   | fraction of cross-sectional area occupied by grain boundaries   |
| $\delta$  | width of a grain boundary (m)   |
| $\tau$  | tortuosity factor for grain boundaries  |
| <b>Properties of a layer of a corona</b>                                |   |
| $A$   | cross-sectional area parallel to layer contacts (m <sup>2</sup> )                                       |
| $N$   | number of grain boundaries per unit length of a traverse parallel to layer contacts (number/m)          |
| $z$   | thickness perpendicular to layer contacts (m)   |
| <b>Quantities in steady-state local-equilibrium modeling of a layer</b> |   |
| $\xi$   | reaction progress (moles PI consumed)   |
| $G$   | growth during unit of reaction progress (m <sup>3</sup> /mol PI consumed)                               |
| $J_i^{\text{model}}$  | flux of component $i$ during unit of reaction progress (moles of the component per mole of PI consumed) |

\* Medium  $k$  = gb (grain boundary) or vol (for volume diffusion).

which gives a maximum estimate because volume diffusion is neglected.

## GEOLOGICAL CONSIDERATIONS

The duration of reaction,  $t$  in Equation 7, must be constrained. Temperature is also important for comparison with other studies. In northeast Scotland (Ashworth and Birdi, 1990) the coronas formed under amphibolite-facies conditions (Kneller and Leslie, 1984: estimated temperature range  $600 \pm 100$  °C), in gabbroic intrusions emplaced during regional metamorphism at approximately 500 Ma. The samples from Norway (Ashworth et al., 1992) are granulites of Precambrian origin, in which the corona reaction was associated with thrust transport of the Jotun Nappe (Ashworth et al., 1992), ending at approximately 395 Ma. The suggested conditions are epidote-amphibolite facies ( $550 \pm 100$  °C). Both field areas show evidence of more complete hydration near fractures, leading to thorough amphibolitization in fault zones or shear zones (Emmett, 1980; Kneller and Leslie, 1984) due to infiltrating fluid.

The time scale of regional cooling and deformation can hardly have been less than 1 m.y. Detailed radiometric work in the Scottish orogenic belt indicates a cooling history lasting tens of millions of years (Dempster, 1985). In northeast Scotland, pegmatites approximately 30 m.y. younger than the gabbro postdate its deformation (Kneller and Leslie, 1984). In Norway, stratigraphic synthesis (Hossack et al., 1985; Hossack and Cooper, 1986) gives a maximum duration of 40 m.y. for the thrusting. Though metamorphic reaction may have outlasted deformation,

TABLE 2. Summary of data and results

|  |                                  |                                  |
|--|----------------------------------|----------------------------------|
| Area   | NE Scotland                      | Jotun Nappe, Norway              |
| Specimen no.   | 53P                              | 359                              |
| Layer  | Hbl                              | Hbl + Qtz                        |
| Layer thickness, $z$ (m)   | $(10 \pm 2) \times 10^{-6}$      | $(10 \pm 4) \times 10^{-6}$      |
| Grain boundary count, $N$ (number/m)   | $(3 \pm 1) \times 10^4$          | $(9 \pm 3) \times 10^4$          |
| Model growth/flux ratio, $G/J_{Al}^{model}$ ( $m^3/mol$ Al)                    | $(9.6 \pm 3.0) \times 10^{-5}$   | $(3.3 \pm 1.8) \times 10^{-4}$   |
| Concentration difference, $\Delta c_{Al}^{eff}$ (moles Al/ $m^3$ )             | $-1.3 \times 10^{(3.5 \pm 0.5)}$ | $-3.2 \times 10^{(2.5 \pm 0.5)}$ |
| Time, $t$ (s)  | $3 \times 10^{(14 \pm 1)}$       | $3 \times 10^{(14 \pm 1)}$       |
| Effective bulk diffusion coefficient: $D_{Al}^{eff}$ ( $m^2/s$ )               | $10^{(-24.4 \pm 1.8)}$           | $10^{(-24.3 \pm 2.1)}$           |
| Assuming dominantly grain-boundary diffusion: $D_{Al}^{gb} \delta$ ( $m^2/s$ ) | $10^{(-28.9 \pm 2.0)}$           | $10^{(-29.3 \pm 2.3)}$           |

Note: Ranges quoted for  $z$  and  $N$  are observed ranges in typical coronas. Uncertainties in  $G/J_{Al}^{model}$ ,  $\Delta c_{Al}^{eff}$ , and  $t$  are discussed in the text. The full ranges for all these quantities are used in calculating the ranges quoted for  $D_{Al}^{eff}$  and  $D_{Al}^{gb} \delta$ ; from Equations 7 and 8.

a time scale exceeding 100 m.y. is very unlikely, because the cooling history in Scotland was essentially over at 400 Ma (Dempster, 1985) and because unmetamorphosed lower and middle Devonian sediments unconformably overlie both uplifted metamorphic belts (Hossack, 1984; Mykura, 1991). To avoid any spurious impression of accuracy, a generous range of uncertainty (1–100 m.y.) is adopted for the time scale available for reaction in both areas. However, the corona-forming reactions require a supply of  $H_2O$  to produce hydrous minerals, so that the true duration of a reaction may be less than the time scale of metamorphic cooling, if  $H_2O$  is available for diffusion from fractures during only a small part of the retrograde history. In this case, the estimates to be derived for diffusion coefficients will be too low. The implications are discussed below.

#### DATA AND NUMERICAL RESULTS

In the coronas of Ashworth and Birdi (1990), the layer sequence is Pl|Hbl + Spl|Hbl|Opx|Ol (Fig. 1). The coronas considered from the study of Ashworth et al. (1992) have the sequence Pl|Ep + Qtz|Hbl + Qtz|Act ± Hbl + Qtz|Cpx. Although only two specimens are considered here, these are typical of their respective localities. The central layer in each sequence is the transition layer (Fig. 1). Table 2 shows values of  $z$  and  $N$  for this layer, measured microscopically, with the range of  $G/J_{Al}^{model}$  computed for the range of fluxes approximately reproducing the modal compositions of the layers.

The hornblende shows slight zoning,  $\Delta c_{Al}^{Hbl}$ , across the layer, which is measurable in favorable cases, such as unusually broad developments of the layer (Mongkoltip and Ashworth, 1983, their Fig. 5a). This is shown in Figure 2 (solid line across the hornblende layer) in terms of Al atoms per formula unit ( $n_{Al}^{Hbl}$ ). It also gives a lower limit for the concentration difference along the grain boundary, the upper limit being one order of magnitude

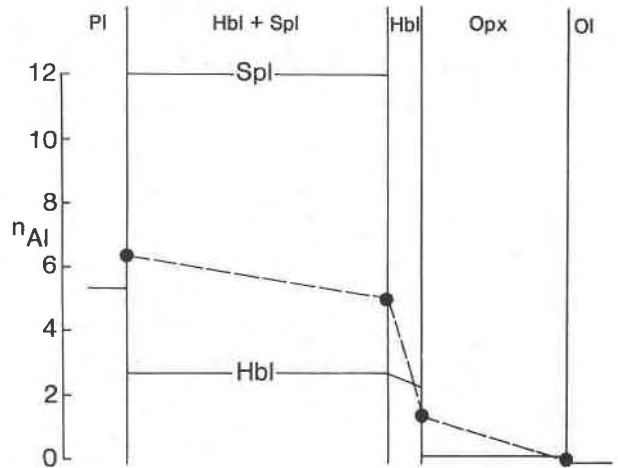


Fig. 2. Approximate Al contents,  $n_{Al}$  atoms per 24-O formula unit of mineral, indicated by typical data for the coronas from northeast Scotland. Relative thicknesses of layers are based on measurements in specimen 53P (Mongkoltip and Ashworth, 1983). The mineral-average model for grain-boundary composition is indicated by solid circles at layer boundaries, connected by dashed lines. The likely concentration difference,  $\Delta c_{Al}^{eff}$ , across the transition layer (Hbl) is considered to be bracketed between this model and the zoning estimated from electron probe data (solid line).

larger according to the following reasoning. Major-element contents in grain boundaries may smooth out some of the disparities between adjacent minerals and successive layers. The Al gradient across the transition layer should not greatly exceed that across the Al-rich layer, through which Al diffusion from the Al-rich reactant mineral is also required by the reactions (Ashworth and Birdi, 1990; Ashworth et al., 1992). A rough model fitting these requirements (dashed lines in Fig. 2) is based on the observation that in bimineralic layers (e.g., Hbl + Spl in Fig. 1) most grain boundaries are shared by both minerals. Thus their average Al content,  $(n_{Al}^{Hbl} + n_{Al}^{Spl})/2$ , gives an initial approximation to the grain-boundary Al content in this layer. The average between this and a typical Al content in the hornblende layer,  $n_{Al}^{Hbl}$ , gives the suggested grain-boundary Al content at the layer contact,  $(3n_{Al}^{Hbl} + n_{Al}^{Spl})/4$ ; analogous averages are suggested at other contacts (solid circles in Fig. 2). In this picture, the difference in Al content across the transition layer accounts for much of the total difference across the corona and is regarded as placing an upper limit on  $\Delta c_{Al}^{gb}$  and hence also on  $\Delta c_{Al}^{eff}$ . Table 2 shows the possible range for  $\Delta c_{Al}^{eff}$  and the range of resulting  $D_{Al}^{eff}$  values from Equation 7.

Diffusion coefficients of other elements are poorly constrained because clear spatial trends in the mineral compositions are not seen. For Si, computed fluxes are also small, indeed zero in the Norwegian example because the assemblages are saturated with respect to  $SiO_2$  (quartz present). For Ca, Mg, and Fe, since mineral compositions indicate that grain-boundary gradients are unlikely to be larger than for Al, the larger fluxes of Mg, Fe (Ashworth

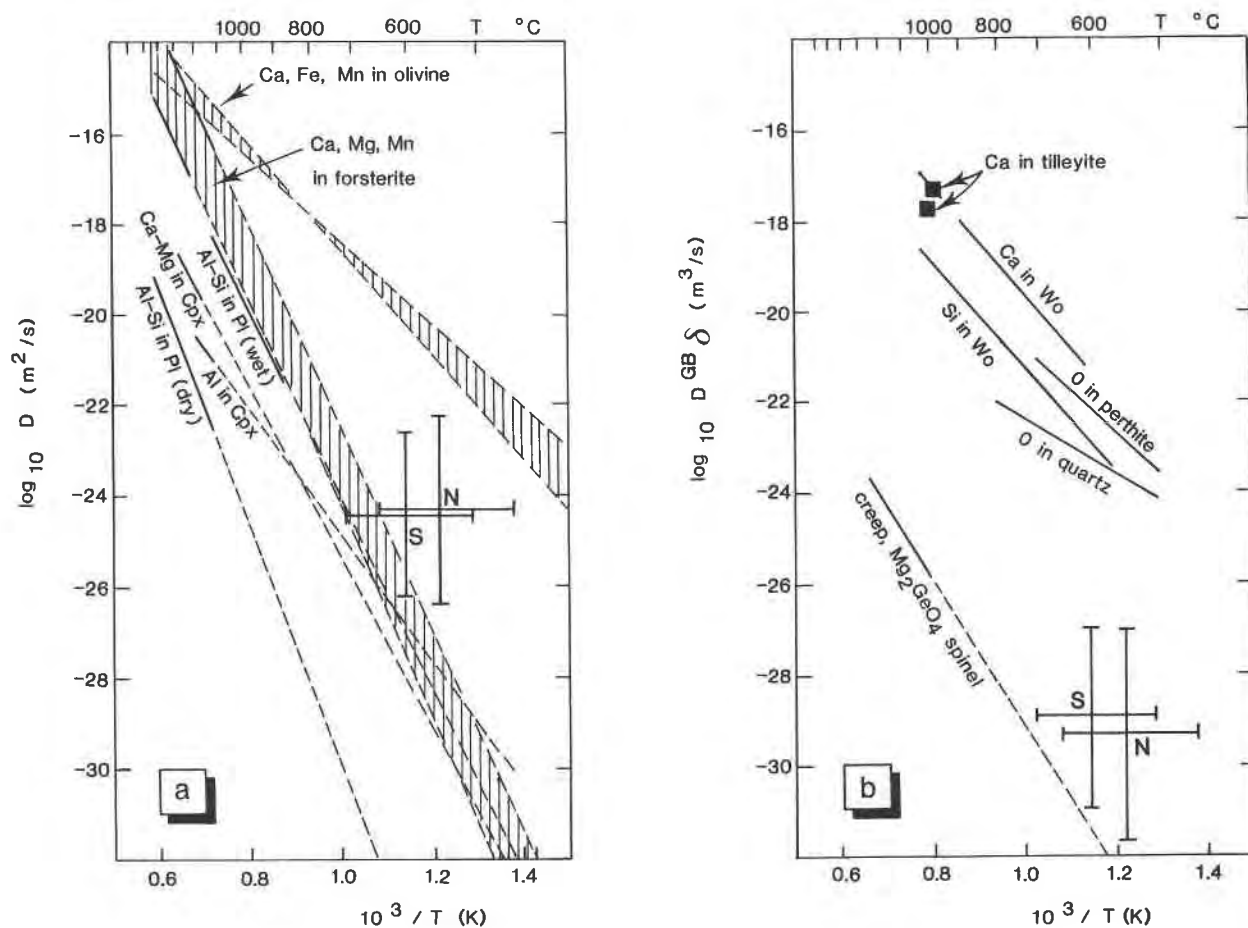


Fig. 3. Estimated kinetic parameters for the areas studied (N = Norway, S = Scotland), compared with data from the literature in Arrhenius diagrams. Dashed lines are extrapolations, from experimental temperature ranges indicated by solid lines. (a) Effective diffusion coefficients from the present study compared with intracrystalline diffusion coefficients from experimental studies. Data for Al-Si diffusion in plagioclase ( $An_{0-26}$ ) under wet conditions ( $H_2O$  deliberately introduced) are from Yund (1986). Similar data for a wider range of plagioclase compositions are presented by Liu and Yund (1992). Other experimental studies are nominally  $H_2O$ -free (dry): Al-Si in plagioclase, Grove et al. (1984); Al in clinopyroxene, Sautter et al. (1988a, 1988b; Sautter, personal communication); Ca-Mg in clinopyroxene, Brady and McCallister (1983); Ca, Mg, and Mn in forsterite, Morioka (1981); Ca, Fe, and Mn in olivine ( $For_{90}$ ) parallel to c, Jurewicz and Watson (1988). (b) Product of grain-boundary diffusion coefficient  $D^{gb}$  and grain-boundary width  $\delta$ . Estimates from the present study are maxima (neglecting volume diffusion). Experimental data on creep deformation of dry  $Mg_2GeO_4$  from Vaughan and Coe (1981) as treated by Rubie (1986). Hydrothermal experimental data for O, in perthite from Nagy and Giletti (1986) and in quartz from Farver and Yund (1991) (1986); inferred natural values for wollastonite and tilleyite from Joesten and Fisher (1988).

and Birdi, 1990), and Ca (Ashworth et al., 1992) indicate  $D_{Al}^{eff}$  at least several times larger than  $D_{Al}^{vol}$ .

#### DIFFUSION KINETICS IN COMPARISON WITH OTHER STUDIES

The two different reactions in different geological settings give consistent estimates for  $D_{Al}^{eff}$ ,  $10^{(-24 \pm 2)}$   $m^2/s$  (Table 2). Operation of grain-boundary diffusion implies  $D_{Al}^{eff} > D_{Al}^{vol}$ . Pure volume diffusion would imply  $D_{Al}^{eff} = D_{Al}^{vol}$ , and the upper part of the range,  $10^{(-23.8 \pm 1.6)}$ , should be preferred because  $\Delta c_{Al}^{vol}$  must be near the low end of the estimated range of  $\Delta c_{Al}^{eff}$  in Table 2. Comparison with experimental volume-diffusion data requires Arrhenius-

law extrapolation from higher temperature experiments (Fig. 3a). Most data for Al refer to Al-Si interdiffusion in plagioclase, which may not be strictly comparable with hornblende, in which some Al is octahedral. There are some data for Al diffusion in clinopyroxene. The comparison is consistent with grain-boundary diffusion, because the  $D_{Al}^{eff}$  estimates are slightly higher than the extrapolated values, even for wet experiments in which  $H_2O$  catalyzes volume diffusion in feldspar (probably through H entering the crystal lattice: Liu and Yund, 1992). Because  $H_2O$  also catalyzes grain-boundary diffusion (Rubie, 1986),  $D_{Al}^{eff}$  for a corona is presumably time averaged over varying values at fluctuating  $H_2O$  contents. Relative

to Al, the greater mobilities of Ca, Mg, and Fe in coronas are comparable with their commonly higher intracrystalline diffusion coefficients (Fig. 3a).

The closeness of extrapolated  $D_{Al}^{vol}$  to  $D_{Al}^{eff}$  estimates in Figure 3a is consistent with pure volume diffusion on a slightly smaller scale than grain-boundary diffusion (as the petrography requires). A measure of volume-diffusion range is  $\sqrt{D_{Al}^{vol}t}$  (e.g., Freer, 1981). Comparably, across the transition layer,  $z \sim \sqrt{D_{Al}^{eff}t}$ , because the factor ( $-2G\Delta c_{Al}^{eff}/J_{Al}^{model}$ ) of Equation 7 is close to unity in both examples. The scale of rim to core Al zoning in some Jotun corona amphiboles ( $\sim 1 \mu\text{m}$ ) is within an order of magnitude of  $z$  ( $\sim 10 \mu\text{m}$ ), suggesting  $D_{Al}^{vol}$  within two orders of magnitude of  $D_{Al}^{eff}$ . It has been mentioned that the  $D_{Al}^{eff}$  estimates are minima because the time scale may have been overestimated if duration of reaction was controlled by  $\text{H}_2\text{O}$  availability for hydration reactions. However, if a time scale many orders of magnitude shorter were invoked, it would imply  $D_{Al}^{eff}$  values higher by the same factor, i.e., no longer comparable with experimentally based estimates of  $D_{Al}^{vol}$ . Thus the results favor long time scales, unless the extrapolated  $D_{Al}^{vol}$  values are too low because a different intracrystalline mechanism comes into effect as temperatures fall below the experimental range, or because hornblende is not comparable with the experimental minerals.

Vance and O'Nions (1990) studied a prograde natural reaction that can be compared with this work. At approximately  $550^\circ\text{C}$ ,  $D^{eff}$  (species unspecified) is estimated to be  $0.4\text{--}6.1 \times 10^{-17} \text{ m}^2/\text{s}$  in rock matrix around growing garnets. Though much higher than the present results, this is regarded as too low to be attributable to diffusion in a fluid (Vance and O'Nions, 1990). Probably, in the prograde reaction, grain-boundary diffusion was assisted by higher  $\text{H}_2\text{O}$  contents than in the coronas.

The  $D_{Al}^{eff}$  values lead to maximum estimates for  $D_{Al}^{gb}\delta$  of  $10^{(-29\pm 2)} \text{ m}^3/\text{s}$  (Table 2) from Equation 8 (volume diffusion neglected). These are consistent with low  $\text{H}_2\text{O}$  content, being just above the minimum entertained by Rubie (1986) for  $\text{H}_2\text{O}$ -bearing solid grain boundaries. Experimental data for dry grain-boundary diffusion extrapolate below the present results (Fig. 3b). Much higher values have been obtained for grain-boundary diffusion in quartz and perthite (Fig. 3b), probably in fluid-absent grain boundaries nearly saturated with dissolved  $\text{H}_2\text{O}$  (Rubie, 1986). These wet experiments measure O isotope diffusion, which is not exactly comparable with cation diffusion, though it is also catalyzed by  $\text{H}_2\text{O}$  (Elphick et al., 1988; Farver and Yund, 1990). The wet experimental results are similar to estimates for natural cation diffusion (Fig. 3b) by Joesten and Fisher (1988). In their very thorough study of contact-metamorphic reaction between chert nodules and surrounding limestone, the diffusion coefficients were estimated indirectly by a method using chemical potential gradients and assuming  $c_i^{gb}$  values similar to  $c_i^{vol}$  in the minerals (Joesten and Fisher, 1988, p. 728). The reactions are prograde decarbonation reactions, e.g., calcite + quartz  $\rightarrow$  wollastonite +  $\text{CO}_2$ , probably in the

absence of aqueous fluid (Olsen et al., 1990), but presumably with  $\text{CO}_2$  dissolved in grain boundaries and possibly with a  $\text{CO}_2$  fluid phase present (Baumgartner et al., 1991; Joesten, 1991, p. 571). Evidently,  $\text{CO}_2$  enhanced the diffusion rates in comparison with the coronas.

## CONCLUSIONS

Despite admittedly large uncertainties, a consistent set of results emerges from the semiquantitative treatment of diffusion in the coronas. The two different reactions give similar estimates for  $D_{Al}^{eff}$  that are compatible with the petrographic evidence for fluid-absent grain-boundary diffusion interacting with volume diffusion. Extrapolation of available experimental data suggests that long time scales ( $> 1 \text{ Ma}$ ) are required to account for the volume diffusion. Implied grain-boundary diffusion rates are much lower than in the prograde,  $\text{CO}_2$ -producing reactions studied by Joesten and Fisher (1988). Estimates of  $D_{Al}^{gb}\delta$  are also lower than expected for highly hydrated grain boundaries (Rubie, 1986). Although  $\text{H}_2\text{O}$  diffused into the rocks to produce hydrous minerals, low contents of dissolved  $\text{H}_2\text{O}$  in the solid grain boundaries are indicated. The small scale of retrograde coronas can be attributed to the retarding effect of low  $\text{H}_2\text{O}$  concentrations on grain-boundary diffusion rates.

## ACKNOWLEDGMENTS

I am indebted to J.B. Brady, S.N. Olsen, and C.T. Foster for thorough criticism of previous drafts.

## REFERENCES CITED

- Ashworth, J.R., and Birdi, J.J. (1990) Diffusion modelling of coronas around olivine in an open system. *Geochimica et Cosmochimica Acta*, 54, 2389–2401.
- Ashworth, J.R., Birdi, J.J., and Emmett, T.F. (1992) Diffusion in coronas around clinopyroxene: Modelling with local equilibrium and steady state, and a non-steady-state modification to account for zoned actinolite-hornblende. *Contributions to Mineralogy and Petrology*, 109, 307–325.
- Baumgartner, L.P., Valley, J.W., and Olsen, S.N. (1991) Extreme isotopic zonation around chert nodules from a contact aureole, Christmas Mountains, TX. *Geological Society of America Abstracts with Programs*, 23, A50.
- Brady, J.B. (1975) Reference frames and diffusion coefficients. *American Journal of Science*, 275, 954–983.
- (1983) Intergranular diffusion in metamorphic rocks. *American Journal of Science*, 283-A, 181–200.
- Brady, J.B., and McCallister, R.H. (1983) Diffusion data for clinopyroxenes from homogenization and self-diffusion experiments. *American Mineralogist*, 68, 95–105.
- Carlson, W.D., and Johnson, C.D. (1991) Coronal reaction textures in garnet amphibolites of the Llano Uplift. *American Mineralogist*, 76, 756–772.
- Dempster, T.J. (1985) Uplift patterns and orogenic evolution in the Scottish Dalradian. *Journal of the Geological Society*, 142, 111–128.
- Elphick, S.C., Graham, C.M., and Dennis, P.F. (1988) An ion microprobe study of anhydrous oxygen diffusion in anorthite: A comparison with hydrothermal data and some geological implications. *Contributions to Mineralogy and Petrology*, 100, 490–495.
- Emmett, T.F. (1980) The geology of the Torfinsbu window, central Jotunheimen, Norway. *Norsk Geologisk Tidsskrift*, 60, 255–261.
- Farver, J.R., and Yund, R.A. (1990) The effect of hydrogen, oxygen, and water fugacity on oxygen diffusion in alkali feldspar. *Geochimica et Cosmochimica Acta*, 54, 2953–2964.



- (1991) Measurement of oxygen grain boundary diffusion in natural, fine-grained, quartz aggregates. *Geochimica et Cosmochimica Acta*, 55, 1597–1607.
- Fisher, G.W. (1973) Nonequilibrium thermodynamics as a model for diffusion-controlled metamorphic processes. *American Journal of Science*, 273, 897–924.
- (1978) Rate laws in metamorphism. *Geochimica et Cosmochimica Acta*, 42, 1035–1050.
- Fisher, G.W., and Elliott, D. (1974) Criteria for quasi-steady diffusion and local equilibrium in metamorphism. In A.W. Hofmann, B.J. Gilletti, H.S. Yoder, Jr., and R.A. Yund, Eds., *Geochemical transport and kinetics*, p. 231–241. Carnegie Institution of Washington Publication 634, Washington, DC.
- Foster, C.T., Jr. (1977) Mass transfer in sillimanite-bearing pelitic schists near Rangeley, Maine. *American Mineralogist*, 62, 727–746.
- (1981) A thermodynamic model of mineral segregations in the lower sillimanite zone near Rangeley, Maine. *American Mineralogist*, 66, 260–277.
- Freer, R. (1981) Diffusion in silicate minerals and glasses: A data digest and guide to the literature. *Contributions to Mineralogy and Petrology*, 76, 440–454.
- Grove, T.L., Baker, M.B., and Kinzler, R.J. (1984) Coupled CaAl-NaSi diffusion in plagioclase feldspar: Experiments and applications to cooling rate speedometry. *Geochimica et Cosmochimica Acta*, 48, 2113–2121.
- Hossack, J.R. (1984) The geometry of listric growth faults in the Devonian basins of Sunnfjord, W Norway. *Journal of the Geological Society*, 141, 629–637.
- Hossack, J.R., and Cooper, M.A. (1986) Collision tectonics in the Scandinavian Caledonides. In M.P. Coward and A.C. Ries, Eds., *Collision tectonics*, p. 287–304. The Geological Society Special Publication 19, London.
- Hossack, J.R., Garton, M.R., and Nickelsen, R.P. (1985) The geological section from the foreland up to the Jotun thrust sheet in the Valdres area, south Norway. In D.G. Gee and B.A. Sturt, Eds., *The Caledonide Orogen—Scandinavia and related areas*, p. 443–456. Wiley, Chichester, U.K.
- Joesten, R.L. (1977) Evolution of mineral assemblage zoning in diffusion metasomatism. *Geochimica et Cosmochimica Acta*, 41, 649–670.
- (1991) Kinetics of coarsening and diffusion-controlled mineral growth. In *Mineralogical Society of America Reviews in Mineralogy*, 26, 507–582.
- Joesten, R., and Fisher, G. (1988) Kinetics of diffusion-controlled mineral growth in the Christmas Mountains (Texas) contact aureole. *Geological Society of America Bulletin*, 100, 714–732.
- Johnson, C.D., and Carlson, W.D. (1990) The origin of olivine-plagioclase coronas in metagabbros from the Adirondack Mountains, New York. *Journal of Metamorphic Geology*, 8, 697–717.
- Jurewicz, A.J.G., and Watson, E.B. (1988) Cations in olivine. Part 2. Diffusion in olivine xenocrysts, with applications to petrology and mineral physics. *Contributions to Mineralogy and Petrology*, 99, 186–201.
- Kneller, B.C., and Leslie, A.G. (1984) Amphibolite facies metamorphism in shear zones in the Buchan area of NE Scotland. *Journal of Metamorphic Geology*, 2, 83–94.
- Liu, M., and Yund, R.A. (1992) NaSi-CaAl interdiffusion in plagioclase. *American Mineralogist*, 77, 275–283.
- Mongkoltip, P., and Ashworth, J.R. (1983) Quantitative estimation of an open-system symplectite-forming reaction: Restricted diffusion of Al and Si in coronas around olivine. *Journal of Petrology*, 24, 635–661.
- Morioka, M. (1981) Cation diffusion in olivine. II. Ni-Mg, Mn-Mg, Mg and Ca. *Geochimica et Cosmochimica Acta*, 45, 1573–1580.
- Mykura, W. (1991) Old Red Sandstone. In G.Y. Craig, Ed., *Geology of Scotland* (3rd edition), p. 297–346. The Geological Society, London.
- Nagy, K.L., and Gilletti, B.J. (1986) Grain boundary diffusion of oxygen in a macroperthitic feldspar. *Geochimica et Cosmochimica Acta*, 50, 1151–1158.
- Nishiyama, T. (1983) Steady diffusion model for olivine-plagioclase corona growth. *Geochimica et Cosmochimica Acta*, 47, 283–294.
- Olsen, S.N., Baumgartner, L.P., and Brown, P.E. (1990) Fluid inclusion study of chert nodules in a contact aureole, Christmas Mountains, Texas. *Geological Society of America Abstracts with Programs*, 22, A347.
- Rubie, D.C. (1986) The catalysis of mineral reactions by water and restrictions on the presence of aqueous fluid during metamorphism. *Mineralogical Magazine*, 50, 399–415.
- Sautter, V., Jaoul, O., and Abel, F. (1988a) Aluminum diffusion in diopside using the  $^{27}\text{Al}(p,\gamma)^{28}\text{Si}$  nuclear reaction: Preliminary results. *Earth and Planetary Science Letters*, 89, 109–114.
- (1988b) Aluminum diffusion in diopside (abs.). *Chemical Geology*, 70, 186.
- Smith, C.S., and Guttman, L. (1953) Measurement of internal boundaries in three-dimensional structures by random sectioning. *Transactions, American Institute of Mining and Metallurgical Engineers*, 197, 81–87.
- Vance, D., and O'Nions, R.K. (1990) Isotopic chronometry of zoned garnets: Growth kinetics and metamorphic histories. *Earth and Planetary Science Letters*, 97, 227–240.
- Vaughan, P.J., and Coe, R.S. (1981) Creep mechanism in  $\text{Mg}_2\text{GeO}_4$ : Effects of a phase transition. *Journal of Geophysical Research*, 86, 389–404.
- Walther, J.V., and Wood, B.J. (1984) Rate and mechanism in prograde metamorphism. *Contributions to Mineralogy and Petrology*, 88, 246–259.
- Yund, R.A. (1986) Interdiffusion of NaSi-CaAl in peristerite. *Physics and Chemistry of Minerals*, 13, 11–16.

MANUSCRIPT RECEIVED AUGUST 19, 1991

MANUSCRIPT ACCEPTED NOVEMBER 20, 1992